Numerical Study of Bubbling Fluidized Beds Operating at Sub-atmospheric Conditions

Lanka Dinushke Weerasiri, Subrat Das, Daniel Fabijanic, William Yang

Abstract—Fluidization at vacuum pressure has been a topic that is of growing research interest. Several industrial applications (such as drying, extractive metallurgy, and chemical vapor deposition (CVD)) can potentially take advantage of vacuum pressure fluidization. Particularly, the fine chemical industry requires processing under safe conditions for thermolabile substances, and reduced pressure fluidized beds offer an alternative. Fluidized beds under vacuum conditions provide optimal conditions for treatment of granular materials where the reduced gas pressure maintains an operational environment outside of flammability conditions. The fluidization at low-pressure is markedly different from the usual gas flow patterns of atmospheric fluidization. The different flow regimes can be characterized by the dimensionless Knudsen number. Nevertheless, hydrodynamics of bubbling vacuum fluidized beds has not been investigated to author's best knowledge. In this work, the two-fluid numerical method was used to determine the impact of reduced pressure on the fundamental properties of a fluidized bed. The slip flow model implemented by Ansys Fluent User Defined Functions (UDF) was used to determine the interphase momentum exchange coefficient. A wide range of operating pressures was investigated (1.01, 0.5, 0.25, 0.1 and 0.03 Bar). The gas was supplied by a uniform inlet at $1.5U_{mf}$ and $2U_{mf}$. The predicted minimum fluidization velocity (U_{mf}) shows excellent agreement with the experimental data. The results show that the operating pressure has a notable impact on the bed properties and its hydrodynamics. Furthermore, it also shows that the existing Gorosko correlation that predicts bed expansion is not applicable under reduced pressure conditions.

Keywords—Computational fluid dynamics, fluidized bed, gas-solid flow, vacuum pressure, slip flow, minimum fluidization velocity.

I. INTRODUCTION

IN the fine chemical industry, the manufactured particulates usually require drying. In some cases, these products include organic solvents that are flammable and pose a risk of explosion with typical fluidized beds. Therefore, the low-oxygen environment of vacuum fluidized beds allows for drying outside of the flammability conditions. Additionally, thermolabile substance can also be dried with vacuum fluidized beds with low risk of material degradation [1]-[4]. Nevertheless, the poor fluidization quality at reduced pressure has been a major detractor [2], [4]. This is also supported by limited experimental and numerical data of such operation.

Lanka Dinushke Weerasiri and Subrat Das are with the Deakin University, Geelong, Australia, School of Engineering (e-mail: dinushke.werrasiri@deakin.edu.au, subrat_das@deakin.edu.au).
Daniel Fabijanic is with the Deakin University, Geelong, Australia, Institute of Frontier Materials (e-mail: daniel.fabijanic@deakin.edu.au).
William Yang is with the CSIRO Process Science and Engineering, Clayton, Victoria, Australia (e-mail: william.yang@csiro.au).

Kawamura and Suezawa [5] were the first to study reduced operating pressure in the range of 0.133 to 13.33 kPa for beds with Group B powders. They found similar fluidization characteristics to atmospheric conditions. The fluidization at low-pressure is markedly different to the usual gas flow patterns of atmospheric fluidization. The gas flow is no longer in the laminar flow regime due to the increase in mean free path of gas molecules. The gas can be molecular state, viscous or intermediate state. The different flow regimes can be characterized by the Knudsen number (Kn) (1). It is a ratio of mean free path of molecules (λ) to the characteristic length (diameter of the solid particle). The mean free path can be calculated from (2) where, K is the Boltzmann constant, T is the temperature, ξ is the diameter of gas molecule and P is the gas pressure [1], [2].

$$Kn = \frac{\lambda}{D} \tag{1}$$

$$\lambda = \frac{KT}{\sqrt{2}\pi\xi^2 P} \tag{2}$$

The gas is described to be in a rarefied or molecular state (also known as Knudsen flow) when a gas flow has a Kn >> 1. The gas particles' collisions are mostly with the container wall rather than with each other. The viscosity of the gas is negligible at this state. Slip flow regime is reached when the mean free path of molecules is comparable to the characteristic length (Kn ≈ 1). The gas flow in this state is characterized by molecular phenomenon and viscosity. In laminar flow (Kn << 1), the characteristic dimension is larger than the mean free path. The gas is governed by the viscosity and the Hagen-Poiseuille law applies.

Generally the pressure drop in a particular bed is expressed by the well-known semi-empirical correlation by Ergun [6]. Ergun [6] reported that the loss of pressure in a fluidized bed was due to both viscous (left term) and kinetic energy losses (right term).

$$\frac{\Delta P}{l} = 150 \frac{u_{mf}(1-\varepsilon_g)^2 \mu_g}{\varepsilon_g^3 \phi^2 d^2} + 1.75 \frac{\rho_s(1-\varepsilon_g)u_{mf}^2}{\phi d} \frac{1}{\varepsilon_g^3} \tag{3}$$

Kusakabe et al. [7] studied fluidization of fine particles at reduced operating pressure. They combined the expressions for throughput of gas in viscous (4) and intermediate (5) flow as put forth by Dushman et al. [8] to propose an expression for minimum fluidization velocity (u_{mf}) (6).

$$Q = \frac{\pi D^4}{128\mu} \frac{PdP}{dx} \tag{4}$$

World Academy of Science, Engineering and Technology
International Journal of Mechanical and Mechatronics Engineering
Vol:13, No:10, 2019

$$Q = \frac{D^3}{6}\sqrt{\frac{2\pi RT}{M}}\frac{dP}{dx} \tag{5}$$

$$u_{mf} = u_{mfv}\frac{P_o}{P}\left[1 + \frac{k_2(1-\varepsilon_{mf})}{\varepsilon_{mf}}\sqrt{\frac{2RT}{\pi M}}\frac{\mu}{\phi dP_o}\right] \tag{6}$$

where, the u_{mfv} is the minimum fluidization velocity for atmospheric pressure; P_o is the measured pressure at the bottom of the bed; P is the pressure at any axial location in the bed; k_2 is a constant 32 [9]; ε_{mf} is the void fraction at u_{mf}; R is the gas constant; T is the gas temperature; M is the molar mass of the gas; μ is the dynamics viscosity of the gas; ϕ is the shape factor and d is the mean diameter of solid particles.

To describe the pressure drop in gas flowing through a granular bed under vacuum pressure, Llop et al. [2] derived a general equation for pressure drop that is valid from Knudsen flow to turbulent flow regime (7). They also derived an expression for determining the minimum fluidization velocity (8).

$$\frac{dP}{dl} = \frac{u}{\frac{16}{45}cos^2\psi\frac{\varepsilon^2\phi d}{(1-\varepsilon)}\sqrt{\frac{2}{\pi\rho P}}+\frac{cos^2\psi\varepsilon^3\phi^2 d^2}{72}\frac{\mu}{\mu(1-\varepsilon)^2}} + 1.75\frac{1-\varepsilon}{\varepsilon^3\phi d}\rho u^2 \tag{7}$$

$$Re_{mf} = \left[\left(\frac{Z}{3.5C_1}\right)^2 + \frac{Ar}{1.75C_1}\right]^{\frac{1}{2}} - \frac{Z}{3.5C_1} \tag{8}$$

$$Z = \frac{1}{\frac{Kn_p}{K_2 C_3}+\frac{1}{K_1 C_2}} \tag{9}$$

$$Ar = \frac{d_p^3\rho g(\rho_s-\rho)}{\mu^2} \tag{10}$$

Zarekar et al. [10] developed a new correlation to predict minimum fluidization Reynolds number (11) for fluidized beds that operate under vacuum and atmospheric gas pressure. They proposed a critical Knudsen number to determine the point at which slip flow term begins to influence the minimum fluidization Reynolds number. They suggested that below the critical Knudsen number, correlations that are developed for atmospheric pressure (based on Ergun equation) are applicable in low operating pressure fluidized beds without the slip flow correction. Equation (12) is a ratio of the minimum fluidization Reynolds number correlation with the same correlation by setting $Kn = 0$.

$$Re_{mf} = -\frac{25.7}{\phi(1+8.8\,Kn)} + \sqrt{\left(\frac{25.7}{\phi(1+8.8\,Kn)}\right)^2 + 0.0365\phi Ar} \tag{11}$$

$$\zeta = \frac{Re_{mf}(Ar,Kn)}{Re_{mf}(Ar,Kn=0)} \tag{12}$$

Computational Fluid Dynamics (CFD) is a widely used technique to predict fluid phenomenon in fluidized beds. The Eulerian-Eulerian continuum model has been well established over the years with many experimental validations [4], [11]-[13]. The CFD approach has been used in predicting complex phenomenon in fluidized beds such as bubble shape, size and growth under various boundary conditions over the years [1], [14]. Four different approaches exist in modelling a fluidized bed: (1) Two-fluid model (TFM) (2) Discrete Particle model (DPM) (3) Discrete bubble model and (4) Molecular Dynamics mode [15]. The TFM method, also known as the Eulerian-Eulerian model, has been the most frequently used modelling approach for gas-fluid fluidized beds with a number of semi-empirical constitutive models [11], [16]. In the Eulerian-Eulerian model, the two phases (granular and fluid phase) are treated as a fully interpenetrating continuum where each phase is modelled as a separate fluid and solved by the Navier-Strokes equation. The coupling of the two phases is given by the interphase momentum exchange coefficient that is given in the momentum balance equation. Fluidized beds have been modelled in 2D [17]-[19] and 3D [20]-[22]. Typically, CFD studies on fluidized beds have used 2D models due to their significantly low computational time. Several authors have reported that 2D models produce similar predictions to 3D models [23]-[25].

The scope of this study was to determine the impact of reduced operating pressure in the range of 1013.25 mbar to 30 mbar on nature of a bubbling gas-solid fluidized bed. In this work, we look at the time-averaged bed properties for Millet particles. The numerical model is validated with the experimental minimum fluidization velocity at reduced pressure.
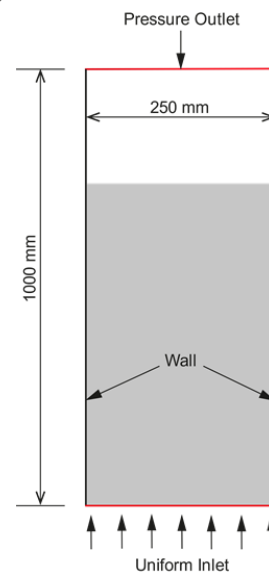
A. Methodology

Fig. 1 Schematic of the computational domain

A two-dimensional fluidized bed (250 x 1,000 mm) was modelled transiently on ANSYS Fluent. Millet particles represented the solid phase with a mean diameter of 1,600 μm and a density of 1,600 kg/m³. Air was used as the fluidizing agent. Gas (air) was introduced from the bottom uniform inlet as shown in Fig. 1. The numerical models were computed for a range of operating pressures (1.01, 0.5, 0.25, 0.1 and 0.03 Bar) and superficial velocities of $1.5U_{mf}$ and $2.0U_{mf}$. For the purpose of this work, we kept the U_{mf} at the value determined

World Academy of Science, Engineering and Technology
International Journal of Mechanical and Mechatronics Engineering
Vol:13, No:10, 2019

for the atmospheric conditions. No slip wall boundary condition was applied for the gas phase with partial slip condition applied to the granular phase with specularity coefficient of 0.5 and coefficient of restitution of 0.9. A structured grid was generated with 2.5, 2.0, 3.0, 4.0 mm cells. Bed expansion was used as the parameter to determine the grid independence. A grid-independent mesh was found for the 2 mm cell mesh.

In Ansys Fluent, the TFM considers each of the fluid phases to be an interpenetrating continua. The conservation equations of mass and momentum are solved for each phase. It is assumed that no mass transfer occurs between the two phases with no heat transfer modelled. Therefore, an isothermal Eulerian-Eulerian approach was used with the particle phase modelled with a constant diameter. The governing equations for incompressible two-phase flow are given below:

Continuity equations
Gas phase:

$$\frac{\partial(\varepsilon_g \rho_g)}{\partial t} + \nabla \cdot \left(\varepsilon_g \rho_g \vec{v_g}\right) = 0 \tag{13}$$

Solid phase:

$$\frac{\partial(\varepsilon_s \rho_s)}{\partial t} + \nabla \cdot \left(\varepsilon_s \rho_s \vec{v_s}\right) = 0 \tag{14}$$

Momentum equations
Gas phase:

$$\frac{\partial(\varepsilon_g \rho_g \vec{v_g})}{\partial t} + \nabla \cdot \left(\varepsilon_g \rho_g \vec{v_g}\vec{v_g}\right) = -\varepsilon_g \nabla P_g + \nabla \cdot \tau_g + \beta_{gs}\left(\vec{v_g} - \vec{v_s}\right) + \varepsilon_g \rho_g \vec{g} \tag{15}$$

Solid phase:

$$\frac{\partial(\varepsilon_s \rho_s \vec{v_s})}{\partial t} + \nabla \cdot \left(\varepsilon_s \rho_s \vec{v_s}\vec{v_s}\right) = -\varepsilon_s \nabla P_g - \nabla P_s + \nabla \cdot \tau_s + \beta_{sg}\left(\vec{v_g} - \vec{v_s}\right) + \varepsilon_s \rho_s \vec{g} \tag{16}$$

where,

$$\tau_g = \mu_g\left[\nabla \vec{v_g} + \nabla^T \vec{v_g}\right] - \frac{2}{3}\mu_g\left(\nabla \cdot \vec{v_g}\right)I \tag{17}$$

$$\tau_s = \mu_s\left[\nabla \vec{v_s} + \nabla^T \vec{v_s}\right] + (\lambda_s - \frac{2}{3}\mu_s)\left(\nabla \cdot \vec{v_g}\right)I \tag{18}$$

$$\varepsilon_s + \varepsilon_g = 1 \tag{19}$$

The granular phase requires closures for the pressure (P_s), shear viscosity (μ_s) and bulk viscosity (λ_s). The granular temperature (Θ) represents the random fluctuation of fluctuating velocity of the solid particles.

$$\frac{3}{2}\left[\frac{\partial(\varepsilon_s \rho_s \Theta_s)}{\partial t} + \varepsilon_s \rho_s \vec{v_s}\Theta_s\right] = (-P_s I + \tau_s) : \nabla \vec{v_s} + \nabla \cdot (k_s \nabla \Theta_s) - \gamma + \phi_s \tag{20}$$

The frictional stress model by Srivastava and Sundaresan [26] has been used in this work:

$$p_c(\varepsilon_s) = \begin{cases} Fr\ \frac{(\varepsilon_s - \varepsilon_{s,min})^r}{(\varepsilon_{s,max} - \varepsilon_s)^s}, \varepsilon_s > \varepsilon_{s,min} \\ 0, \varepsilon_s \le \varepsilon_{s,min} \end{cases} \tag{21}$$

$$\mu_s^f = \frac{p_c(\varepsilon_s)\sqrt{2}\sin\emptyset}{2\varepsilon_s\sqrt{\overline{D}_{ij}:\overline{D}_{ij} + \frac{\Theta_s}{d_s^2}}} \tag{22}$$

where, D_{ij} is the strain rate and $\emptyset$ is the internal angle of friction.

$$\gamma = 3(1 - e^2)\varepsilon_s^2 \rho_s g_o \Theta_s(\frac{4}{d_s}\left(\frac{\Theta_s}{\pi}\right)^{\frac{1}{2}} - \nabla \cdot \vec{V_s}) \tag{23}$$

The drag force acting on a particle in a gas-granular system is represented using the interphase momentum exchange coefficient (F_s). Several drag models are available to predict the interphase exchange coefficient [1], [27]-[29]. The Gidaspow drag model [27] has been the most widely used in the past literature. It is a combination of drag laws developed by Ergun [6] for dense phase and Wen and Yu [28] for dilute phase. Later Llop et al. [2] derived a pressure drop equation (7) that takes into account the losses at slip flow and later Kumar et al. [1] extended this work by deriving the interphase exchange coefficient (25) for the dense phase. The Slip flow model is implemented into ANSYS Fluent as a UDF.

$$\frac{dP}{dl} = \frac{F_s}{\varepsilon_g}\left(\vec{v_g} - \vec{v_s}\right) \tag{24}$$

$$F_s = \frac{1 - \varepsilon_g}{(0.1356)\ \phi\ d_s\sqrt{\frac{1}{\rho P} + \frac{1}{150}\frac{\alpha_g}{(1-\varepsilon_g)\mu_g}(\phi d_s)^2}} + 1.75\frac{\rho_g(1-\varepsilon_g)(\vec{v_g}-\vec{v_s})}{\phi d_s} \tag{25}$$

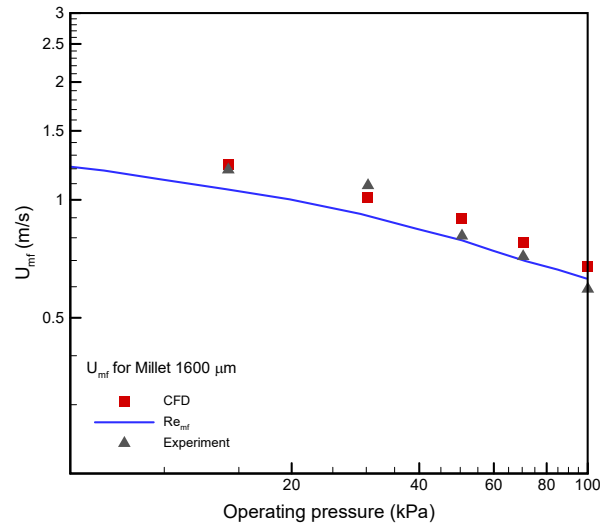## II. RESULTS AND DISCUSSION

Fig. 2 Minimum fluidization velocity at reduced pressure

In order to establish the validity of the numerical model, a numerical study has been conducted to determine the minimum fluidization velocity of millet particles at reduced pressure. The minimum fluidization velocity was determined

World Academy of Science, Engineering and Technology
International Journal of Mechanical and Mechatronics Engineering
Vol:13, No:10, 2019

using a pressure drop vs. superficial velocity plot. The pressure drop within the bed was tracked transiently and average over time. The method followed here is further explained in [30]. Fig. 2 shows that the predicted minimum fluidization shows good agreement with the experimental data from Llop et al. [2] with an average error of 8.7%.

A. Effect of Pressure on Bubbling Behavior

The simulation data were time-average for 10 s of flow time in order to capture the average properties of the bed. The cut-off for the dense phase has been taken as $\varepsilon_g < 0.8$. The bubbles were found to grow from the superficial inlet and the rise along the bed. They were notably larger at higher superficial velocity. The trajectory of the bubbles was mostly away from the centerline of the bed similar to the observations by Saxena [31] for shallow beds. This is reflected in the porosity in the bed shown in Fig. 3. The observed bubbles were found to be elongated shape as they rise in the bed. The bubbles were also found to increase in size by the process of coalescence with other bubbles and entrainment of gas from the bed. However, as the operating pressure was reduced, the size of bubble reduced until no bubbles were seen. This ultimately reduces the porosity in the bed as seen in Fig. 3. The rational for this behavior is due to the rise in minimum fluidization velocity as the pressure is reduced. A number of authors have experimentally and numerically discussed this behavior [2], [7], [30], [32]. Llop et al. [2] developed correlation that was found to predict minimum fluidization velocity with good agreement with the experimental data. Two equations were derived for sharp (27) and spherical particles (). Given that the millet particles have a shape factor of 0.9, (26) is used to predict the minimum fluidization velocity. Fig. 4 shows that our bubbling velocity of fixed $1.5U_{mf}$ and predicted minimum fluidization velocity is similar when the pressure is at 190.75 mbar. This validates the bubbling behavior of the bed that was seen when the pressure was reduced.
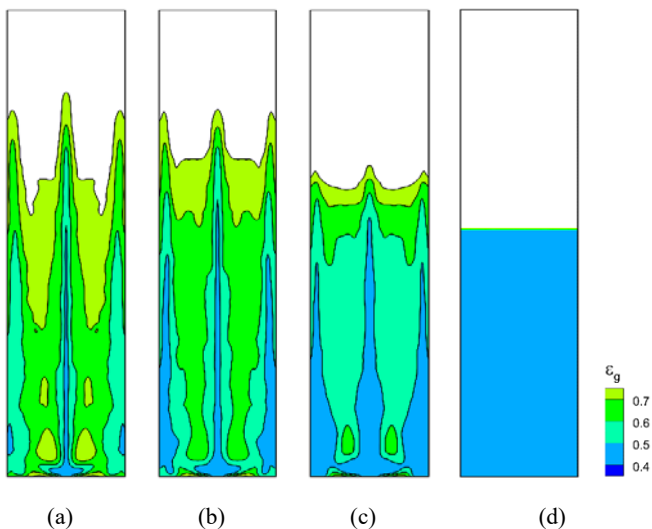
Round powders ($\phi > 0.8$):

$$Re_{mf} = \left[\left(\frac{0.909}{Kn_p + 0.0309}\right)^2 + 0.0357 Ar\right]^{1/2} - \frac{0.909}{Kn_p + 0.0309} \tag{26}$$

Sharper powders ($0.5 < \phi \ll 0.8$):

$$Re_{mf} = \left[\left(\frac{1.9}{Kn_p + 0.0492}\right)^2 + 0.0571 Ar\right]^{1/2} - \frac{1.9}{Kn_p + 0.0492} \tag{27}$$
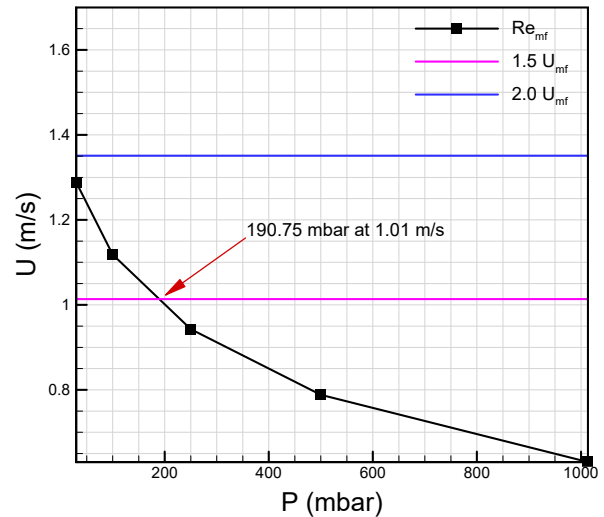

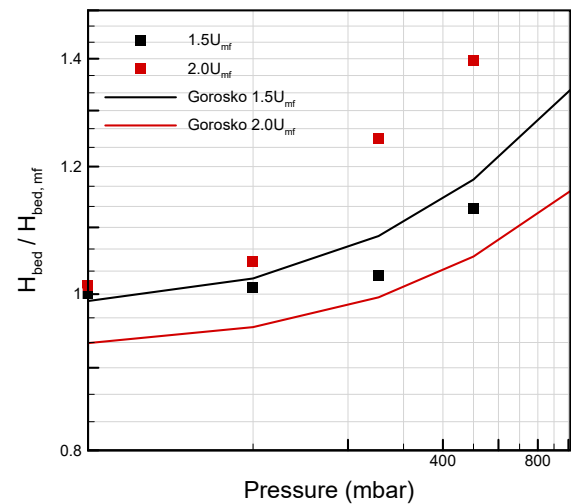Fig. 4 Gas superficial velocity at varying operating pressure

Fig. 5 Bed expansion ratio at varying operating pressure and superficial velocity

B. Bed Expansion

The bed expansion is defined as a ratio of the expanded bed height over the bed height at minimum fluidization velocity. The bed height was measured up to the cells with $\varepsilon_g = 0.8$ as the interface between the bed and freeboard. Fig. 5 shows that the bed expansion reduces with reduction in pressure. The bed expansion ratio reaches a similar value ($\approx 1\%$) at 0.03 bar for both 1.5 and 2.0 Umf superficial velocity. We also calculated

Fig. 3 Time-average void fraction contour at $2U_{mf}$ with (a) 1.01 (b) 0.5 (c) 0.25 and (d) 0.1 Bar pressure

World Academy of Science, Engineering and Technology
International Journal of Mechanical and Mechatronics Engineering
Vol:13, No:10, 2019

the bed expansion using the Gorosko correlation [33] for porosity given in (28). The relation between the porosity and bed expansion is given in (29). The predicted bed expansion with Gorosko correlation at the reduced pressures is shown in Fig. 5. The inaccuracy is higher at increased superficial velocity. The impact of the reduced pressure on the gas properties were included in the calculation of the correlation, however, this correlation was not developed to predict the porosity of fluidized bed's at reduced pressure conditions.

$$\varepsilon = \left(\frac{18 Re_o + 0.36 Re_o^2}{Ar} \right) \qquad (28)$$

$$\frac{H_{bed}}{H_{mf}} = \frac{1 - \varepsilon_{mf}}{1 - \varepsilon} \qquad (29)$$

III. CONCLUSION

We have performed an investigation into the impact of vacuum pressure on bubbling beds with a numerical model. The numerical model was validated with experimental minimum fluidization velocity at reduced pressure. The model predicted that operating pressure has a significant impact on the bubbling characteristics of the bed and bed expansion ratio. The numerical model accounted for the changes in gas properties and slip flow conditions with the implementation of the slip flow drag model. The Gorosko correlation was found not to accurately represent the bed expansion.

REFERENCES

[1] A. Kumar, P. Hodgson, D. Fabijanic, and W. Gao, "Numerical solution of gas–solid flow in fluidised bed at sub-atmospheric pressures," *Advanced Powder Technology,* vol. 23, no. 4, pp. 485-492, 2012/07/01/ 2012.

[2] M. F. Llop, F. Madrid, J. Arnaldos, and J. Casal, "Fluidization at vacuum conditions. A generalized equation for the prediction of minimum fluidization velocity," *Chemical Engineering Science,* vol. 51, no. 23, pp. 5149-5157, 1996/12/01/ 1996.

[3] A. Kumar, P. Hodgson, W. Gao, S. Das, and D. Fabijanic, "Investigating the effect of segregation of particles and pressure gradient on the quality of fluidisation at sub-atmospheric pressures," *Powder Technology,* vol. 254, pp. 137-149, 2014/03/01/ 2014.

[4] S. Zarekar, A. Bück, M. Jacob, and E. Tsotsas, "Numerical study of the hydrodynamics of fluidized beds operated under sub-atmospheric pressure," *Chemical Engineering Journal,* vol. 372, pp. 1134-1153, 2019/09/15/ 2019.

[5] S. Kawamura and Y. Suezawa, "Mechanism of gas flow in a fluidized bed at low pressure," 化学工学 vol. 25, no. 7, pp. 524-530, 1961.

[6] S. Ergun, "Fluid flow through packed columns," *Chem. Eng. Prog.,* vol. 48, pp. 89-94, 1952 1952.

[7] K. Kusakabe, T. Kuriyama, and S. Morooka, "Fluidization of fine particles at reduced pressure," *Powder Technology,* vol. 58, no. 2, pp. 125-130, 1989/06/01/ 1989.

[8] S. Dushman, J. M. Lafferty, and R. Pasternak, "Scientific foundations of vacuum technique," *Physics Today,* vol. 15, p. 53, 1962.

[9] S. Dushman, *Scientific Foundations of Vacuum Technique.* John Wiley and Sons, Inc., New York, 1949.

[10] S. Zarekar, A. Bück, M. Jacob, and E. Tsotsas, "Reconsideration of the hydrodynamic behavior of fluidized beds operated under reduced pressure," *Powder Technology,* vol. 287, pp. 169-176, 2016/01/01/ 2016.

[11] A. Kumar, P. Hodgson, W. Gao, D. Fabijanic, and S. Das, "Drag models comparison by single injection in vacuum fluidised beds," in *ICMF 2013: Proceedings of the International Conference on Multiphase Flow*, 2013, pp. 1-6: ICMF.

[12] J. A. M. Kuipers, W. Prins, and W. P. M. Van Swaaij, "Numerical calculation of wall-to-bed heat-transfer coefficients in gas-fluidized beds," *AIChE Journal,* vol. 38, no. 7, pp. 1079-1091, 1992.

[13] A. Kumar, S. Das, D. Fabijanic, W. Gao, and P. Hodgson, "Bubble–wall interaction for asymmetric injection of jets in solid–gas fluidized bed," *Chemical Engineering Science,* vol. 101, pp. 56-68, 2013/09/20/ 2013.

[14] A. Kumari, P. Hodgson, W. Gao, D. Fabijanic, and S. Das, "Drag models comparison by single injection in vacuum fluidised beds," in *ICMF 2013: Proceedings of the International Conference on Multiphase Flow*, 2013, pp. 1-6: ICMF.

[15] A. Kumar, "Investigations into hydrodynamics and heat transfer in vacuum fluidised beds," Deakin University, 2014.

[16] Y. Wang, Z. Zou, H. Li, and Q. Zhu, "A new drag model for TFM simulation of gas–solid bubbling fluidized beds with Geldart-B particles," *Particuology,* vol. 15, pp. 151-159, 2014/08/01/ 2014.

[17] B. G. M. van Wachem, J. C. Schouten, R. Krishna, and C. M. van den Bleek, "Eulerian simulations of bubbling behaviour in gas-solid fluidised beds," *Computers & Chemical Engineering,* vol. 22, pp. S299-S306, 1998/03/15/ 1998.

[18] B. G. M. van Wachem, J. C. Schouten, R. Krishna, and C. M. van den Bleek, "Validation of the Eulerian simulated dynamic behaviour of gas–solid fluidised beds," *Chemical Engineering Science,* vol. 54, no. 13, pp. 2141-2149, 1999/07/01/ 1999.

[19] H. Enwald, E. Peirano, A. E. Almstedt, and B. Leckner, "Simulation of the fluid dynamics of a bubbling fluidized bed. Experimental validation of the two-fluid model and evaluation of a parallel multiblock solver," *Chemical Engineering Science,* vol. 54, no. 3, pp. 311-328, 1999/02/01/ 1999.

[20] V. Verma, J. T. Padding, N. G. Deen, and J. A. M. Kuipers, "Numerical Investigation on the Effect of Pressure on Fluidization in a 3D Fluidized Bed," *Industrial & Engineering Chemistry Research,* vol. 53, no. 44, pp. 17487-17498, 2014/11/05 2014.

[21] W. Zhong, M. Zhang, B. Jin, and Z. Yuan, "Flow behaviors of a large spout-fluid bed at high pressure and temperature by 3D simulation with kinetic theory of granular flow," *Powder Technology,* vol. 175, no. 2, pp. 90-103, 2007/06/06/ 2007.

[22] A. Acosta-Iborra, C. Sobrino, F. Hernández-Jiménez, and M. de Vega, "Experimental and computational study on the bubble behavior in a 3-D fluidized bed," *Chemical Engineering Science,* vol. 66, no. 15, pp. 3499-3512, 2011/08/01/ 2011.

[23] N. Xie, F. Battaglia, and S. Pannala, "Effects of using two- versus three-dimensional computational modeling of fluidized beds: Part I, hydrodynamics," *Powder Technology,* vol. 182, no. 1, pp. 1-13, 2008/02/15/ 2008.

[24] T. W. Asegehegn, M. Schreiber, and H. J. Krautz, "Influence of two- and three-dimensional simulations on bubble behavior in gas–solid fluidized beds with and without immersed horizontal tubes," *Powder Technology,* vol. 219, pp. 9-19, 2012/03/01/ 2012.

[25] S. Cloete, S. T. Johansen, A. Zaabout, M. van Sint Annaland, F. Gallucci, and S. Amini, "The effect of frictional pressure, geometry and wall friction on the modelling of a pseudo-2D bubbling fluidised bed reactor," *Powder Technology,* vol. 283, pp. 85-102, 2015/10/01/ 2015.

[26] A. Srivastava and S. Sundaresan, "Analysis of a frictional–kinetic model for gas–particle flow," *Powder Technology,* vol. 129, no. 1, pp. 72-85, 2003/01/08/ 2003.

[27] D. Gidaspow, R. Bezburuah, and J. Ding, "Hydrodynamics of circulating fluidized beds: kinetic theory approach," Illinois Inst. of Tech., Chicago, IL (United States). Dept. of Chemical Engineering1991.

[28] C. Y. Wen and Y. H. Yu, "Mechanics of fluidization," in *Chemical Engineering Progress Symposium Series*, 1966, vol. 62, pp. 100-111, 1966.

[29] M. Syamlal and T. J. O'Brien, "Computer simulation of bubbles in a fluidized bed," in *AIChE Symp. Ser*, 1989, vol. 85, no. 1, pp. 22-31: Publ by AIChE.

[30] L. Weerasiri, V. Kumar Panangipalli, S. Das, and D. Fabijanic, "Predicting Minimum Fluidization Velocity For Vacuum Fluidized Beds," presented at the 3th International Conference on CFD in the Minerals and Process Industries, Melbourne, Australia, 2018.

[31] S. C. Saxena, "Heat Transfer between Immersed Surfaces and Gas-Fluidized Beds," in *Advances in Heat Transfer*, vol. 19, J. P. Hartnett and T. F. Irvine, Eds.: Elsevier, 1989, pp. 97-190.

[32] M. F. Llop and N. Jand, "The influence of low pressure operation on fluidization quality," *Chemical Engineering Journal,* vol. 95, no. 1, pp. 25-31, 2003/09/15/ 2003.

[33] L. Mörl, S. Heinrich, and M. Peglow, "Chapter 2 Fluidized bed spray granulation," in *Handbook of Powder Technology*, vol. 11, A. D. Salman, M. J. Hounslow, and J. P. K. Seville, Eds.: Elsevier Science B.V., 2007, pp. 21-188.